Received: 24 August 2021 | Revised: 14 October 2021 | Accepted: 25 October 2021

DOI: 10.1002/mmce.22963

REVIEW ARTICLE

INTERNATIONAL JOURNAL OF RF AND MICROWAVE COMPUTER-AIDED ENGINEERING WILEY

Recent advancement in the design of mixers for software-defined radios

Shilpa Mehta[1] | **Xue Jun Li**[1] | **Massimo Donelli**[2]

[1]Department of Electrical and Electronic Engineering, Auckland University of Technology, Auckland, New Zealand

[2]Department of Civil, Environmental and Mechanical Engineering, University of Trento, Trento, Italy

Correspondence
Shilpa Mehta, Department of Electrical and Electronic Engineering, Auckland University of Technology, Auckland, 1010, New Zealand.
Email: shilpa.mehta@aut.ac.nz

Abstract

The implementation of software-defined radio necessitates a versatile radio frequency (RF) front-end that can support multiple standards in different frequency bands. This article presents the state-of-the-art multiband and wideband mixers in the context of different receiver architectures suitable for software-defined radio (SDR). Wideband and multiband mixer designs reported in the literature are categorized on the basis of their circuit architecture. This study tabulates the results of mixer designs with an emphasis on noise figure (NF), conversion gain (CG), linearity, and image rejection ratio. The best parameters reported in the comparison are 68–84 dB of CG, 3.2 dB of NF, 2.5 mW of power consumption, 12.5 dBm of third-order input intercept point, and 0.015 mm^2 of area at different frequencies. The study also discusses the design challenges and techniques to overcome those issues. The article concludes with the summary and prospective developments for SDR architectures.

KEYWORDS

mixer, reconfiguration, software-defined radios, wireless communication

1 | INTRODUCTION

Wireless communications have been around since the early 1990s, which subsequently brought up many standards and application areas such as in civil, military, and medical industries. With technological advancement, the number of wireless standards has been increasing.[1] Consequently, it is desired to design a radio front-end that can support multiple wireless standards.[2–5] This was difficult or even impossible for the traditional radios because of their hardware dependency. On the contrary, software-defined radio (SDR)s have the ability to reconfigure their operation.[6–11] In a conventional SDR receiver, after analog-to-digital conversion (ADC), most signal processing was carried out within the digital domain through field-programmable gate arrays (FPGAs).[12,13] This approach maximally enabled the software-controlled feature of SDRs. However, it led to high power consumption, which formed the bottleneck that prevented the wide adoption of SDRs. Additionally, some hardware components (mixers, amplifiers, and antenna) are also required that are not completely replaceable by their software counterparts.

An alternative approach to implement SDR is to use discrete-time and mixed-signal systems where the mixing process occurs before ADC. Besides, a power-scalable ADC is utilized, which is capable of providing tunable resolution and bandwidth. This approach was proven to be successful as they provide good reconfigurability with low-power consumption.[10] Mixers are used to alter the frequency of the electromagnetic signal while maintaining all other characteristics of the original signal such as phase or

amplitude. The main purpose of frequency conversion is to enable amplification of the received signal at a frequency other than radio frequency (RF).[14,15]

As mixers are the important blocks of the receiver circuit, the overall performance of the receiver gets affected by the mixer's performance. Therefore, for good SDR receiver performance, a mixer is required to have low noise figure (NF), high conversion gain (CG), good linearity, and high image rejection ratio (IRR), while consuming small die/chip areas.

This survey aims to provide a timely summary of the recent development of mixers for SDRs. Section 2 discusses the mixer fundamentals, followed by the design topologies in Section 3. Section 4 focuses on the mixer specifications, followed by the wideband and multiband mixers for the SDR receivers in Section 5. Section 6 discusses the impedance matching techniques used in multiband mixers for SDR and Section 7 provides a comparative study of different mixers. Section 8 discusses the design challenges, and finally, Section 9 concludes the survey with future developments.

2 | MIXER FUNDAMENTALS

A mixer is one of the key components in a transceiver, and it can shift the signal from one frequency to another. Figure 1 illustrates the operation of a mixer. Upon mixing, the frequency of the output signal is in the form of a sum or difference of those of the input signals due to the presence of two input signals. In transmitters, mixers can perform frequency upconversion to shift intermediate frequency (IF) to RF. Similarly, in receivers, mixers can perform frequency downconversion to shift RF to IF.[17]

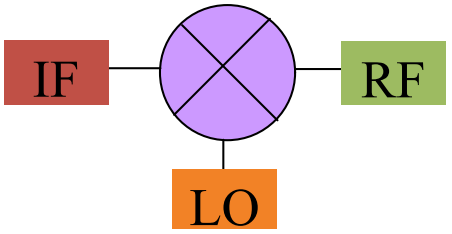

(A) Upconversion mixer

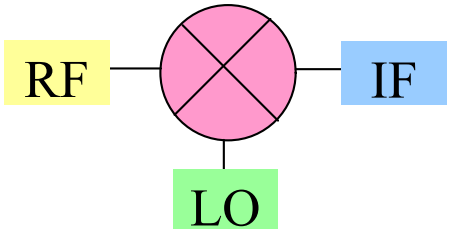

(B) Downconversion mixer

FIGURE 1 Mixers conversion[16]

For good performance with low NF, high linearity, polarity switching through local oscillator (LO) input is required. Such a mixer will have RF signal divided into in-phase and out-of-phase parts; the conversion switch operated by LO signal can alternatively choose in-phase and out-of-phase signals. Ideally, mixers will introduce the minimum amount of noise and have good linearity.[18] Moreover, they should be independent of LO amplitude and intermodulation products. However, practical mixers have the following limitations: non-negligible NF, limited CG, and linearity.[19] For the sake of convenience, we focus on conversion mixers in this survey.

3 | MIXER DESIGN TOPOLOGIES

Mixers are broadly classified as passive mixers and active mixers as shown in Figure 2. For passive mixers, they will introduce signal attenuation. The mixing is achieved through passive switches. Therefore, the switches are turned on and off depending on the LO signal, which is compared to a reference voltage and mixing is achieved through the multiplication operation of RF and LO frequency signals (in terms of square wave or sinewave). Passive mixers are widely used because of their simplicity, zero power consumption, high third order input intercept point (IIP3), and good NF at the expense of port isolation. However, their main drawback is the high LO power requirement.[17]

Different from passive mixers, active mixers can provide high CG, good port isolation, low NF, and low LO

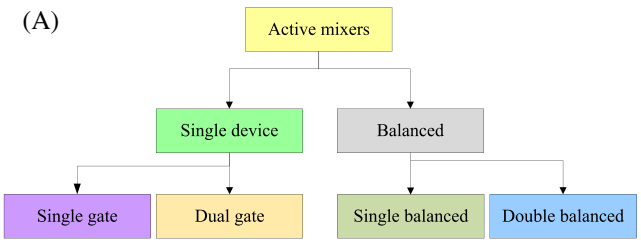

Active mixers classification

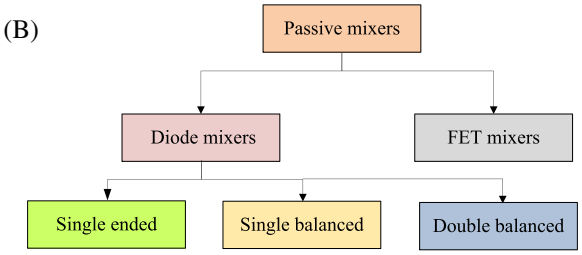

Passive mixers classification

FIGURE 2 Mixers

power requirements. However, it is difficult for them to achieve good linearity without the use of additional circuitry.

3.1 | Passive mixers

Passive mixers can be implemented using nonlinear diodes or field-effect transistors (FETs).

3.1.1 | Passive diode mixers

The mixers adopt nonlinear diodes and filtering elements. As shown in Figure 3, they can be subdivided into single-ended, single-balanced, and double-balanced mixers, respectively.

1. As shown in Figure 3A, single ended mixers do not require DC power supply and are easy to implement. However, they do require filtering elements to improve the port isolation.[17]
2. Single-balanced mixers employ two devices, which are often implemented as two single-device mixers linked by 180° or 90° couplers. If a 90° coupler is used within the mixer circuitry, matching networks must be employed, but port isolation will be reduced. The 180° couplers, on the other hand, provides good port isolation but matching will be poor. Based on this concept, a single-balanced mixer circuit is proposed as shown in Figure 3B.[20] The circuitry contains a 90° hybrid coupler, two Schottky diodes, matching circuitry, and a bandpass filter. The LO input signal is divided within two Schottky diodes. Similarly, the RF input signal is equally divided at the Schottky diode with a phase difference. After mixing of RF and LO signals within these diodes, the outputs obtained are combined at the IF. Thus, to filter out the desired frequency component at the output, the bandpass filters are used. Balanced mixers can provide improved port isolation compared to single-ended mixers. However, they require larger LO input power.
3. As shown in Figure 3C, double-balanced mixers contain differential inputs and outputs. The switching operation of mixers depend on the LO signal behavior (positive and negative cycles). During this operation, the left-hand and right-hand pair diodes alternatively switch on and off and the nodes "a" and "c" refer to the virtual ground for RF. The points "b" and "d" refer to the balanced RF signal, which connects to other points alternatively. Such mixers can cover a wideband and attain high linearity at the expense of elevated NF.[21]

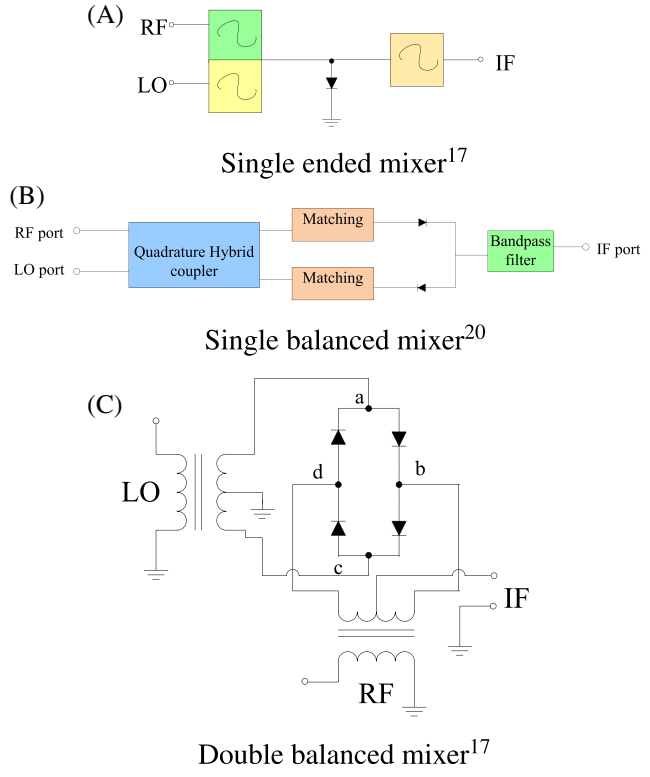

FIGURE 3 Passive mixers

3.1.2 | Passive FET mixers

As shown in Figure 4, passive FET mixers employ FETs as switches. In passive FET mixers, drain-source resistance acts like a voltage-controlled resistor, where the channel resistance is a function of gate-source voltage. During positive half-cycles, two FETs M_1, M_3 are enabled and M_2, M_4 are disabled. Thus, IF balun secondary winding gets connected to that of RF balun through switched on FETs. The reverse operation occurs during the

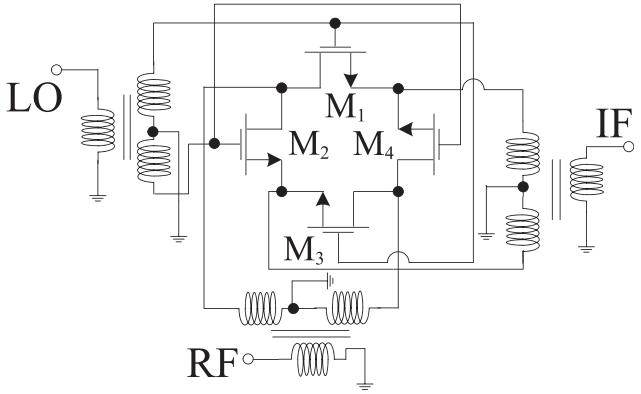

FIGURE 4 Passive FET quad mixer.[22] FET, field-effect transistor

negative half cycle and the reverse polarity RF input reaches the IF output. The frequency of FET switching operation is determined by the LO signal frequency.[22] Passive FET mixers outperform diode mixers in terms of linearity with similar CGs. To conclude the section, a comparative summary of passive mixers is provided in Table 1. Table 1 shows that for high linearity performance, a double balanced passive diode mixer or passive FET mixer can be used. Likewise, single-ended mixers can be used for simple architecture, and for wideband operation double balanced passive mixers can be used.[17]

3.2 | Active mixers

Active mixers can be classified as single device active mixers and balanced active mixers.

3.2.1 | Single device active mixers

Single-device mixers are further subdivided into single gate and dual gate mixers, as shown in Figure 5A,B, respectively.

1. Single gate mixers use a single transistor to take RF and LO inputs through the gate. Therefore, diplexing is needed to distinguish both inputs.[17]
2. Dual gate mixers use dual-gated transistors to take RF and LO signals through separate gate terminals, resulting in good port isolation and IIP3.[17]

3.2.2 | Balanced mixers

Balanced mixers are further grouped into single-balanced and double-balanced (Gilbert) mixers, as shown in Figure 6A,B, respectively.

1. Single-balanced mixers adopt single-ended RF input and differential LO inputs, leading to a differential IF output signal as shown in Figure 6A. These mixers attain good CG, low NF, and high port isolation. Moreover, they consume less power due to small area as compared to double-balanced mixers.[23]
2. Gilbert mixers adopt differential inputs and output as shown in Figure 6B. These mixers combine two single-balanced mixers to achieve better performance

TABLE 1 Comparison of passive mixers

	Passive diode mixers			
Category	**Single-ended mixer**	**Single-balanced mixer**	**Double-balanced mixer**	**Passive FET mixer**
Benefits	High-frequency band operation	Rejection of poor responses and intermodulation products	Wideband operation	High linearity
	Easy to design and inexpensive	Improved port isolation	High linearity and reasonable NF	$\frac{1}{f}$ flicker noise is not induced
	Good input linearity and low noise	Rejection of AM noise in LO	High port isolation	
	Low LO drive while using integrated LO buffers		Improved suppression of spurious products	
Drawbacks	Poor port isolation	Requires high LO drive level	Requires high LO drive level	Requires DC bias to correct diode switching
	Poor 2nd-order distortion	To reduce the overall NF both diodes must be well matched	Requires at least two baluns	Mixers with discrete components require optimization for performance improvements
	Require off-chip diplexers for separating RF and IF ports		For bandwidth improvement, pad attenuators must be included	
	Requires injection filter for attenuating LO's AM noise		Improper matching leads to high CL	

Abbreviations: AM, amplitude modulation; CL, conversion loss; FET, field-effect transistor; LO, local oscillator; NF, noise figure.

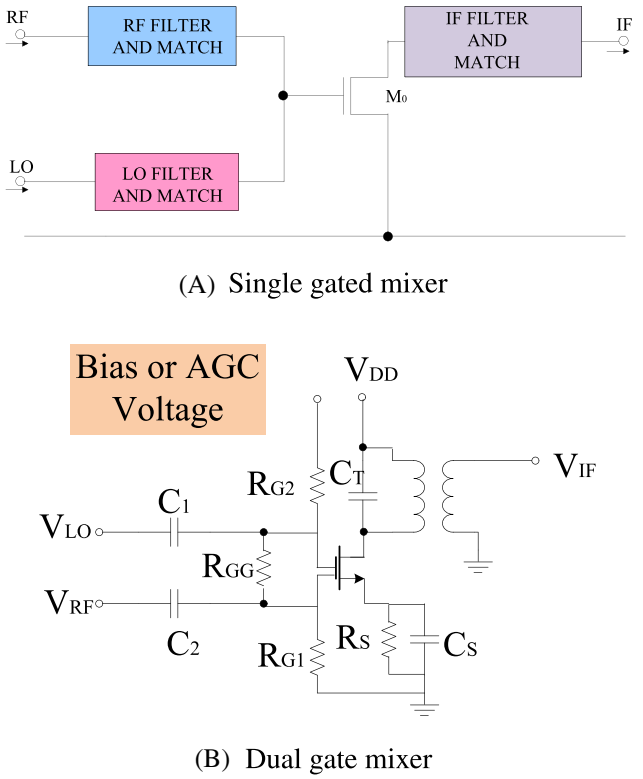

FIGURE 5 Single device active mixers[17]

in terms of IIP3, port isolation, and CG.[17] RF stage transistors (operating in saturation mode) are used to convert RF input voltage to current and hence amplify it. The transistors (operating in triode mode) connected to the LO stage are used for switching operation. The LO signal voltage must be higher than the RF signal voltage for proper operation.

4 | PERFORMANCE METRICS OF MIXERS

Mixers play an important role in wireless communication systems, especially in superheterodyne receivers.[24–33] Therefore, to characterize mixer performance, metrics should be selected carefully. But, there exists a trade-off among different performance parameters like CG, NF, IIP3, and power consumption. High CG mixers experience high NF, whereas high IIP3 can be achieved by sacrificing CG and power consumption.[23]

Port isolation can be accomplished using mixer balance and hybrid junctions. Thus, it is important to maximize the isolation as the undesired signal dissipates RF power and may affect the required output signal. It may also cause electromagnetic interference.[34]

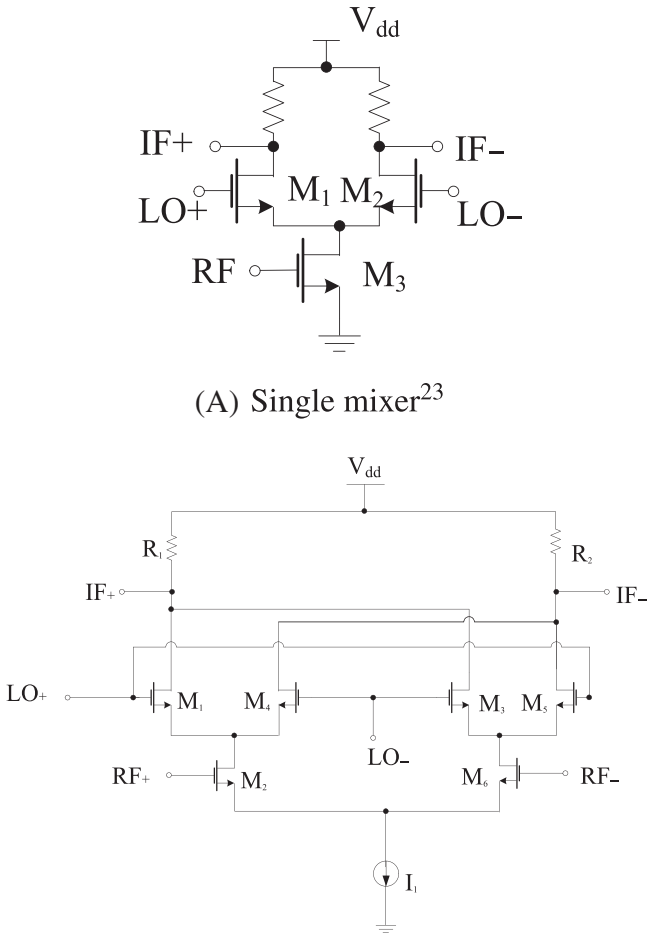

FIGURE 6 Active balanced mixers

Image rejection must be considered while designing any mixer as the unwanted signal present at the same input port may generate the false output signal. This will lead to wasted power consumption.[35]

Impedance matching refers to the extent of matching between source and load impedance. Improper matching may lead to reflection and filters are required to avoid distortion at the receiving end.[36]

To measure the performance of a mixer, vector network analyzers (VNAs) with calibration advancements can be used, including scalar mixer calibration (SMC) and vector mixer calibration (VMC). To perform SMC, the frequency offset introduced by mixer must be taken into account. For this purpose, VNA will provide input IF or RF that will be upconverted or downconverted to the desired frequency at the mixer output. As the output frequency at VNA Port 2 differs from the input frequency at Port 1, Port 2 must be set to frequency-offset mode. SMC uses conventional Short-Open-Load-Thru (SOLT) calibration, with the condition that the calibration must account for all frequencies of interest. SOLT calibration

measurements can be done over both supplied frequency ranges when the frequency-offset mode is enabled. Although this approach is time consuming, it provides accurate results. Another approach is to perform SOLT measurement by disabling frequency-offset mode. This approach quickly generates the calibration results. However, it ends up in interpolation when actual measurements are taken. In addition to the mixer-under-test, VMC also requires another calibration mixer and filter. VMC calibration depends on the frequency conversion process. Although SMC setup is simpler compared to VMC, VMC calibration is important in phase and group delay measurement.[38] With the technology advancement, SDR mixers emerged to handle multiple standards with different frequencies in a concurrent or discrete manner.[39] Table 2 summarizes the specifications of these mixers as per SDR applications. SDR mixers should satisfy these specifications for all supported bands[40] without affecting circuit size, power consumption compared to narrowband mixer designs, making them suitable for mobile applications.

5 | DESIGN TECHNIQUES

As shown in Figure 7, SDR mixers can be broadly categorized as wideband and multiband mixers. Wideband mixers face the difficulty to attenuate interfering signals (especially for harmonics).[42] Therefore, multiband mixers are needed for the SDR. One of the easiest solutions for multiband is to use several mixers in parallel, each operating at different bands. However, this approach leads to complex mixer designs with high power consumption and large circuit size. Thus, the preferred solution is to design a single mixer, which is robust enough to operate at different standards without significantly affecting the performance.

5.1 | Wideband mixers

Wideband mixers demonstrate flat gain response across a wideband for different applications. Additionally, they require tuning circuits for frequency reconfiguration. Some of the common wideband mixer topologies include cross-coupled common gate,[37] inductive peaking,[41,43,44] bulk cross-coupling, and current bleeding[45] and current reuse with the current mirror approach.[2]

Figure 8 shows cross-coupled common gate transconductance stage with a wide LO-based Gilbert mixer. It can achieve flat CG with good matching and low-power consumption. However, it suffers from high NF and low IIP3. Alternatively, an inductive peaking technique can be used. Conventional approaches use an inductor with cross-coupled PMOS transistors (CCPT), diode connected NMOS transistors (DC-NT) dependent IF load to enhance the load impedance, while maintaining high transconductance and hence CG. The inductive peaking will balance the CG drop at higher frequencies while improving the bandwidth.[43,46] Figure 9 shows the use of an inductive peaking topology at the transconductance stage

TABLE 2 SDR reconfigurable mixer specifications

Parameters	Explanation	Typical values
Conversion gain	Ratio of O/P power to I/P power	>10 dB
Noise figure	NF = $10\log_{10}$(F), where $F = \mathrm{SNR_{in}}/\mathrm{SNR_{out}}$	<5 dB
Linearity	Relation between I/P and O/P	≥0 dBm
Reverse Isolation	Power leakage from one port to another	<−30 dB
Image rejection ratio	Ratio of O/P from desired to O/P from image signals	>20 dB
Return loss	Losses from port reflections	<−10 dB
Area	On-chip area	<2 mm^2
Bandwidth	Wide spectrum operation	>500 MHz
Frequency reconfiguration	Operating frequency modification	Multiple bands

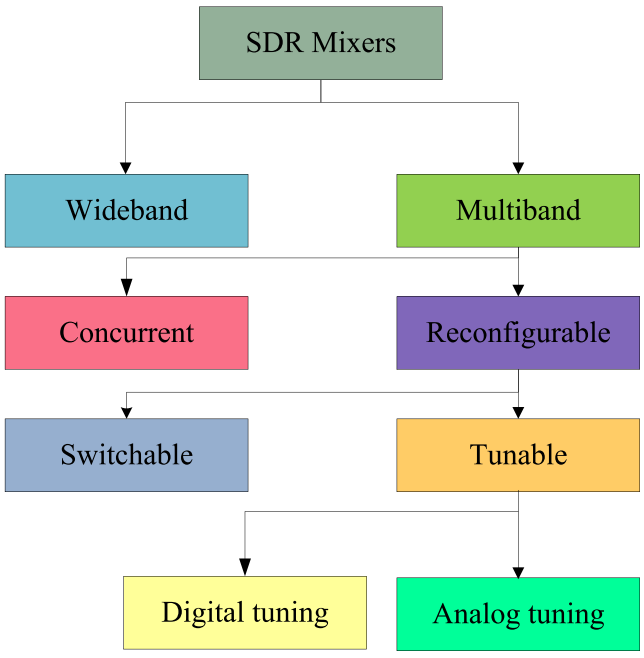

FIGURE 7 Classification of SDR Mixers

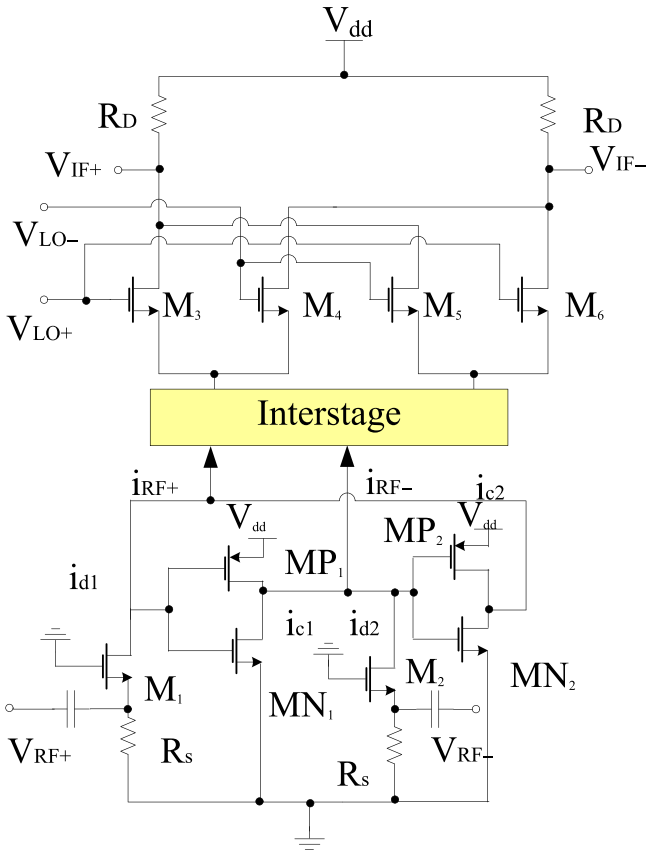

FIGURE 8 Cross-coupled mixer[37]

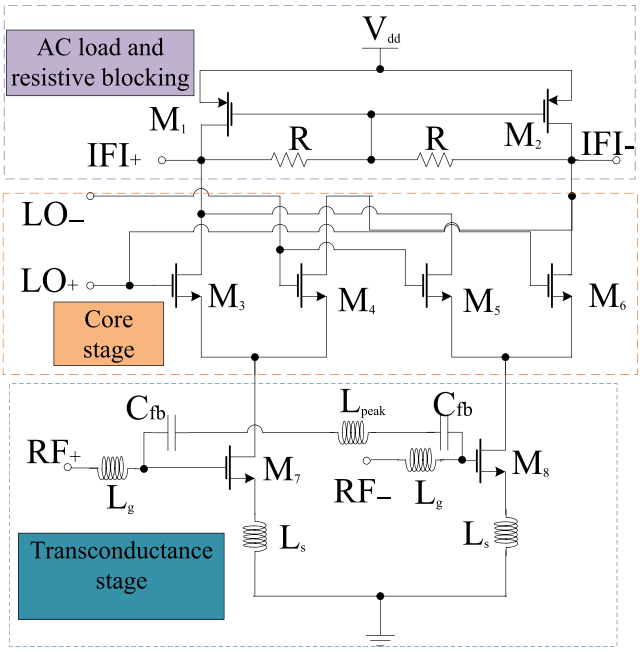

FIGURE 9 Wideband mixer[41]

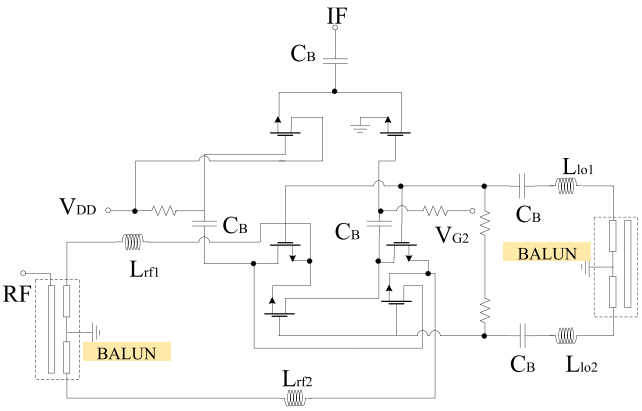

FIGURE 10 Wideband CMOS mixer[44]. CMOS, complementary metal–oxide–semiconductor

to provide wideband impedance matching.[41] The technique is employed to resonate with the parasitic capacitors leading to a large and flat gain. In the design, the load stage consists of large resistances followed by the transistors acting like diode loads to provide a virtual AC ground at the gates of the transistors, leading to high voltage headroom affecting the overall NF and IIP3 performance. Yang et al. utilized a resistive double-balanced structure that attained good IIP3 and CG as shown in Figure 10.[44] In the design, on-chip baluns are developed to meet single to differential transformation requirements. Besides, inductors are placed in the RF signal path between the balun and mixer core for optimizing input matching. Likewise, for obtaining high and wideband gain, the optimum gate and source inductive feedback technique is employed.

5.1.1 | Active wideband mixers

Gilbert topology is well known for providing high CG, good port isolation.[49–53] Adiseno et al. proposed a Gilbert mixer with flat CG, but the design suffers from high NF and low IIP3.[54] Although the design is suitable for compact, low IF receivers, the overall power consumption is high.

To maintain high CG and high IIP3 simultaneously, an active and resistive combined topology can be used, which is convenient for direct receiver architectures with low-power consumption.[55] Solati et al. employed derivative superposition and noise cancelation approach for the mixer circuitry.[56] For linearity enhancement purposes, auxiliary transistors have been used. Additionally, a novel linear path with multiple gated transistor topology has been introduced for the thermal noise cancelation of the input transistors. The design achieved not only high CG and high IIP3, but also low NF.

Active mixers show a trade-off between CG-NF. Ma et al. employed current reuse and current mirror techniques while designing a mixer, resulting in high CG, high IIP2 at the expense of NF.[2]

Another design challenge is to simultaneously maintain large bandwidth and high CG. Blaakmeer et al. proposed a blixer circuitry, which is basically introduced as a combination of low noise amplifier (LNA), Balun, and I/Q mixer.[57] The proposed design is compact with low-power consumption. Hamed et al. adopted a novel passive balun for a mixer that uses a multi-dielectric layered structure for a broadband operation within coplanar structure.[58] The design attained high return loss, while maintaining high CG and bandwidth as well.

5.1.2 | Passive wideband mixers

Passive mixers can be used for low voltage operation as they can provide high IIP3 because of linear channel resistance.[59–62] Murphy et al. proposed a noise-canceling receiver with an eight-phase passive mixer.[63] With the employment of passive mixers and high-gain baseband operational amplifiers, the virtual ground behaves ideally and also suppresses voltage swing prior to baseband filtering. As with the rise in mixer phases, the noise folded from high-order harmonics was suppressed, leading to better NF. In addition, in the presence of fixed transimpedance amplifier outputs, desired signal I/Q components can be attained and the undesired signal components are canceled. Namsoo et al. proposed a resistively degenerated mixer, which achieved low NF, high IIP3, and low-power consumption.[64]

5.1.3 | Dual topology mixer

Active mixers are good for attaining high CG and passive mixers can attain high IIP3. Therefore, to attain high performance in CG and IIP3 simultaneously, one solution is to combine active and passive mixers in one design.[65] The design uses an active RF stage and passive core stage while utilizing the current mirror technique[2] without degrading the overall performance.

SDR mixers based on dual topology mixers require compact mixers that provide high performance and consume low power while operating within a wideband. Existing mixers with on-chip inductors suffer from problems like large chip area, low-quality factor, and susceptible to electromagnetic interference within unified systems. For wideband SDR mixers, capacitive parasitics associated with CMOS transistors need extra attention because they affect the CG and NF performance, especially within complex designs. Although there is a possibility to tune them with on-chip inductors, off-chip inductors prove to be a better solution that maintains low area requirement without performance degradation.[66]

5.2 | Multiband mixers

Multiband mixers can handle multiple bands simultaneously with continuous or discrete tuning.[67] They can be further classified as concurrent mixers and reconfigurable mixers.

5.2.1 | Concurrent mixers

Concurrent mixers can receive different frequency bands concurrently. However, to satisfy the miniaturization and low-cost needs, low-power consumption should be emphasized as most of the power consumption comes from mixers and amplifiers within the receiver circuit. Likewise, the design complexity should be reduced. Therefore, a single mixer with multiple operational bands will be beneficial.[68,69] Similar work proposed mixers operating in dual bands by utilizing capacitive tuning for multiband operation and attaining a high IRR.[69]

Noise-canceling designs were proposed by utilizing current bleeding and transistor-based attenuation[30] to attain high CG and low NF. Likewise, the mixer switching approach in[70] can also be used for dual-band concurrent operation. Chen et al. proposed a concurrent dual-band LNA with a dual-band subharmonic mixer.[71] This approach eliminated the need for multiple frequency synthesizers for the receiver and hence reduced the overall manufacturing cost. The overall CG and NF were good at the expense of linearity.

Abdelrheem et al. presented a dual-band impedance matching network for concurrent narrowband matching at two frequencies and a resistive degeneration approach for performance improvement.[47] The design achieved a small chip area because of the utilization of off-chip

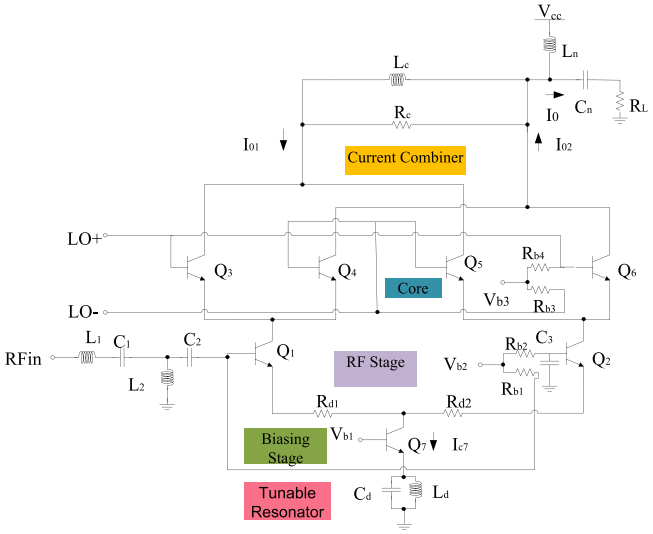

FIGURE 11 Dual-band mixer[47]

passive components. As shown in Figure 11, Q_1, Q_2 transistors form an RF stage and Q_3–Q_6 form transistors of the core stage and Figure 12 shows the return loss which is >10 dB within the entire band. The design also attains high CG within dual bands. It was found that transconductance is large for the frequencies smaller than unity-gain frequency f_T, which makes it easier for a mixer to operate at more than one frequency. Therefore, the obtained transconductance, G_m can be defined by:

$$G_m = g_m/2(1+g_m R_d), \quad (1)$$

where G_m refers to the driving stage, g_m is the small-signal transconductance, and R_d refers to the degeneration resistance, respectively.

It is not necessary to use off-chip components to reduce the overall area of a mixer design. On-chip filters/resonators/components can be used to provide high performance while reducing the overall cost of the circuitry. Wang et al. have proposed the design that adopted both on-chip baluns and LC series–parallel resonator.[72] The resonator circuitry helps to operate within dual bands. The proposed mixer consumed low power at the expense of degraded CG and NF performance. Nevertheless, it attained high port isolation.

Hsu et al. proposed a novel concurrent dual-band receiver employing dual-band LNA, stacked mixer, voltage-controlled oscillator, and variable gain amplifiers.[48] The design adopted the current-reuse approach. Thereafter, for power reduction purposes, it adopted a common gain stage and component stacking. The design attained high CG and low NF with low-power consumption. Figure 13 shows the concurrent dual-band receiver circuitry, where a parallel–series combination-matching network was proposed for concurrent matching. The complete design covered a moderate chip area, including matching networks and pads. Its return loss is >10 dB in both bands as shown in Figure 14. The design also attained good CG at the desired concurrent bands.

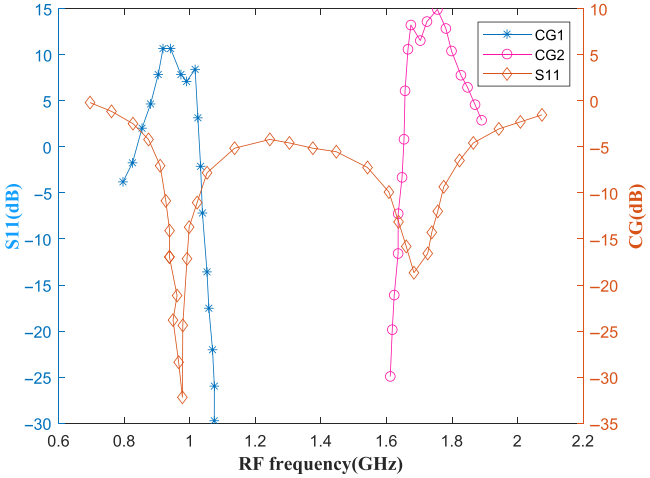

FIGURE 12 Performance metrics of dual-band mixer[47]

5.2.2 | Reconfigurable mixers

High-performance reconfigurable mixers are desired to support different bands of operation. The conventional way of designing reconfigurable mixers for multiband applications is to integrate mixers in parallel, each operating within a different band. However, they are limited to lower frequency bands. The reconfigurable mixers can be classified as switchable mixers and tunable mixers.

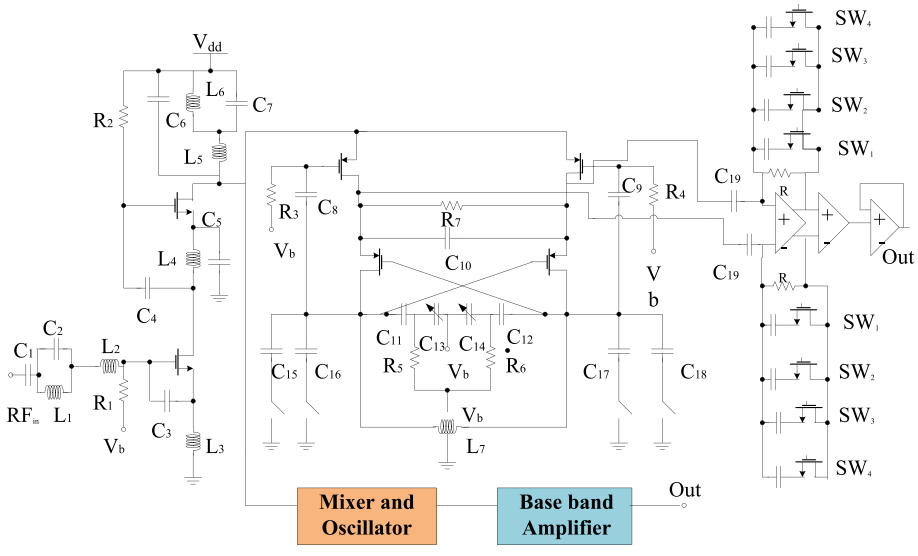

FIGURE 13 Concurrent dual-band receiver[48]

Switchable mixers

Switchable mixers can operate within different bands using switches. The reconfiguration can be possible at different frequencies by toggling the switches, which are discrete in nature. The resultant frequency bands have the highest return loss. One of the switchable mixers is shown in Figure 15, which is based on the Gilbert cell approach. The parasitic capacitor of the switching stage (LO stage) is the main factor for the small dynamic range that is tuned with spiral inductors, programmable inductors developed using transformers, or small spirals at different frequencies. The switches presented in the filter section allow switching at different frequencies. However, to control the programmable inductors, NMOS varactors are also employed within the filter circuitry. The programmable inductor section is shown in Figure 15. The input impedance is inductive and the effective impedance can be expressed as

$$L_e(w) = L_1 + (i_2/i_1)M, \tag{2}$$

L_1, L_2, and M are the primary, secondary, and mutual inductance, respectively. k is the magnetic coupling coefficient. With the variation in C_2, the current ratio varies and hence the effective inductance. Generally, the programmable inductor is employed for tuning the parasitic capacitors to enhance the loading impedance to improve the noise performance and the second-order intermodulation distortion. The overall design covered a large chip area while attaining good performance in terms of CG, NF, and IIP3.

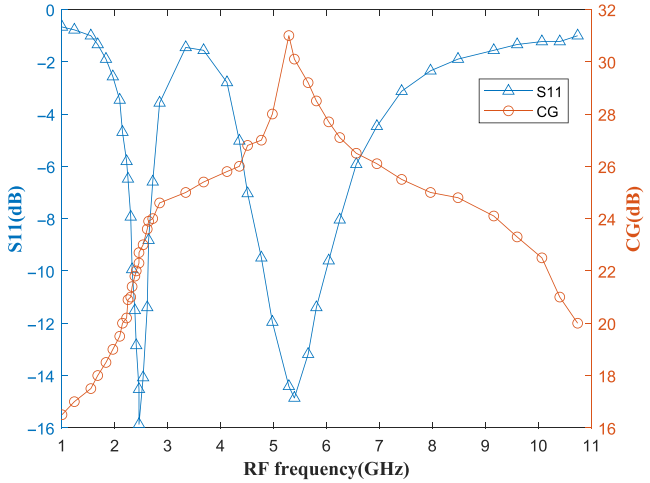

FIGURE 14 Performance metrics of concurrent dual-band receiver[48]

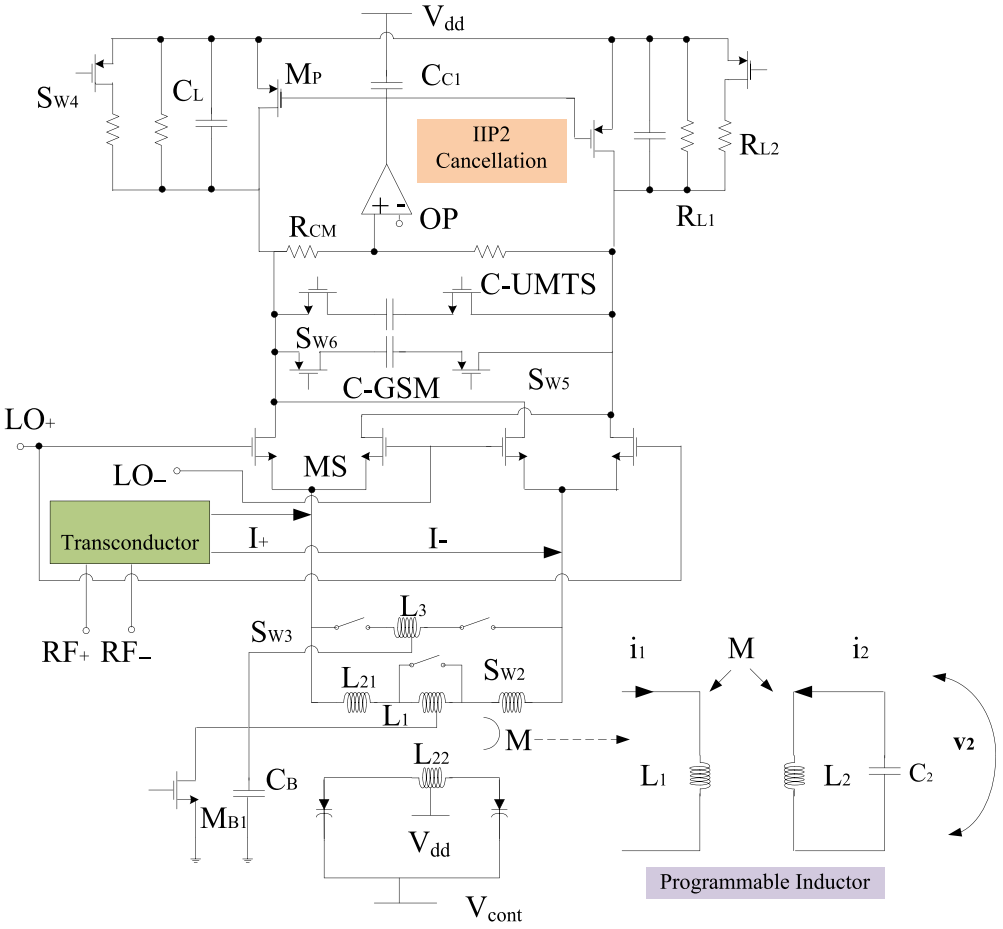

FIGURE 15 Reconfigurable mixer[73]

Similarly, Cao et al. proposed current driven passive mixer and switchable transconductance array to attain low flicker noise and good IIP3.[74] The buffer section is designed using the Tow-Thomas transimpedance biquad amplifier as a filter. The switchable amplifier is responsible for providing high wideband gain. The mixer section as shown in Figure 16 is designed using a passive mixer because of its ability to provide high linearity and low flicker noise. To further enhance the performance, threshold variation is taken into consideration with the help of the DC bias voltage controlling process for every transistor gate within the circuitry, resulting in high DC offset. Therefore, to overcome this issue, digital to analog converters are added at the IF end that helps in the DC offset calibration process.

Tunable mixers

Tunable mixers can be tuned at different frequencies within a band, continuously or discretely. In general, digitally tunable SDR receivers employ multiband mixers for broadband frequency range coverage.[75] Channelization and waveform detection is possible with different encoding schemes along with frequency hopping that makes use of digital signal processing algorithms and FPGAs. The work refers to digital receiver capability to perform ADC sampling and FPGA-based digital down-conversion (DDC) process.[76]

A frequency-tuning algorithm was discussed by Ibrahim et al.[77] The proposed algorithm in the work utilized a platform consisting of universal software radio peripheral and RFX2400 daughterboard. This FPGA-based DDC approach allows lossless signal processing. For example, FPGA devices are commonly used for digital signal processing and communication with the advancement in SDR technology. This is mainly because of their reconfiguration capability.[78,79]

For SDR receivers, RF front-ends operate in a wideband. During the selective filtering process, out-of-band blockers (strong carriers beyond the digital receiving band) and harmonic interference are amplified as the desired signal, which degrades the SNR. Some SDR receivers rely on the voltage-mode passive mixer to provide filtering for the suppression of out-of-band blockers, but they are not effective to suppress harmonic interference. Fortunately, this can be done with harmonic rejection mixers. However, the gain and phase mismatch leads to the degradation of the harmonic rejection ratio (HRR). Therefore, the gain and phase must be calibrated if high HRR is required, although the calibration is a tedious task.

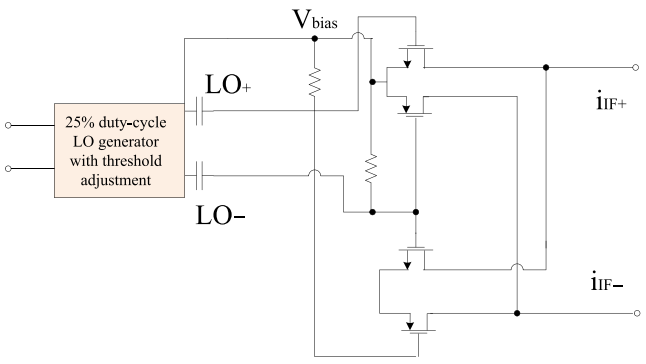

FIGURE 16 The current driven passive mixer[74]

Different techniques can be used to improve the HRR at the expense of CG and phase mismatching. Harmonic rejection approaches consume high power due to complicated circuit and large die area.[80] For a high IRR, good CG, and low-power consumption, the mixer proposed by Zhang et al. can be chosen.[81] It featured a zero/low IF variable SDR structure that uses digital calibration for both narrowband and wideband purposes. Three modes were considered. For low NF performance, a current-mode mixer was used. Additionally, for high linearity performance, a voltage passive mixer was utilized specifically for out-of-band rejection. Then, the harmonic rejection passage was used for vector gain calibration. However, it only supports a limited number of bands with degraded CG, NF, and linearity.[81] As such, continuous tuning is preferred over discrete tuning, as the former is less sensitive to process variations.

5.2.3 | Active multiband mixers

Several approaches have been discussed in the literature for attaining high CG and NF performance. Different mixers were developed and proposed by Douss et al., based on current bleeding and charge injection approaches.[3] However, they may lead to high power consumption and degraded CG.[65] Additionally, the mixer was proposed by Fan et al. that used Tow-Thomas topology as a filter to achieve high performance without degrading CG, NF, and IIP3.[28] The mixer proposed by Chen et al. is a good example to adopt the current reused G_m stage, source degeneration, and multi-gated transistor approaches.[59] The design attained high IIP3 at the expense of CG and NF. Similarly, Qin et al. proposed a mixer with an improved complimented common gate pair as the RF stage.[82] The proposed design also used a transformer for chip area reduction and PMOS with inductive peaking better for current bleeding. This improved the NF, CG, and bandwidth performance at the expense of IIP3.

Other than the above-mentioned approaches, the use of RLC tunable resonators[16] helps in attaining high CG and low NF, as shown in Figure 17. The resonance frequency is known as

$$f_r = 1/\left(2\pi\sqrt{LC}\right). \quad (3)$$

The design achieved low NF and good CG as shown in Figure 18. Nevertheless, there is always a trade-off among CG, NF, and IIP3.

5.2.4 | Passive multiband mixers

Yang et al. showed that passive mixers dependent on power amplifier degeneration can be used to lower the NF without additional switching requirements.[83] Although the proposed design was fully reconfigurable, the power consumption was quite high. Thus, this design is not suitable for low-power SDR applications. Likewise, Sowlati et al. proposed a transceiver to include a passive mixer while maintaining low phase noise and better port isolation.[84] The design also covers low area and attains high CG. Both inductor-based and inductorless designs can cover large chip area. An inductorless I/Q mixer was proposed by Poobuapheun et al., which employs an operational amplifier-based output section with a passive core stage.[85] The proposed mixer attained high CG, high IIP3, and good NF at the expense of chip area.

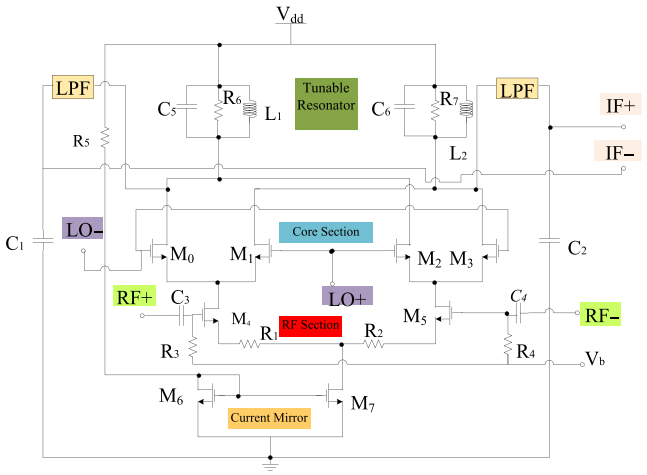

FIGURE 17 Tunable Gilbert mixer[16]

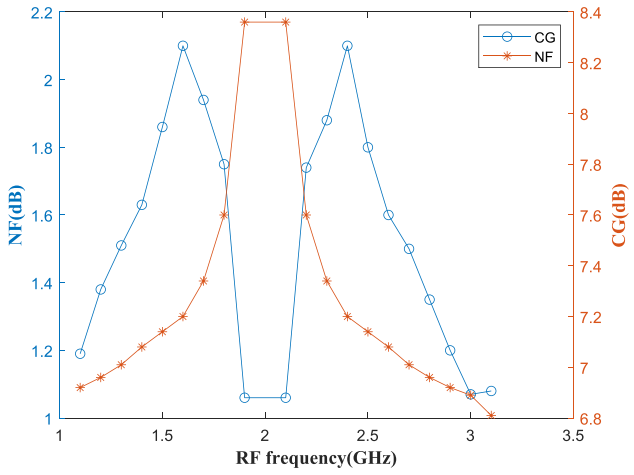

FIGURE 18 Performance metrics of tunable mixer[16]

5.2.5 | Dual-mode multiband mixers

Passive mixers are highly linear with low-power consumption. However, they suffer from high conversion loss and need a large LO power. On the contrary, active mixers can provide better CG and require small LO power. However, they suffer from low linearity and high NF.[86] To the best of our knowledge, the mixer proposed by Nguyen et al. is the first dual-mode mixer designed using an active balun coupled ring mixer that can alternatively work as an active and passive mixer.[87] In their design, the CG control was possible by varying the control voltage. The design of active balun was using a DC-coupled differential pair approach to eliminate off-chip IF balun. In high CG mode, the design attained moderate IIP3, while, in low CG mode the linearity performance is better.

6 | IMPEDANCE MATCHING TECHNIQUES

Conventional mixer circuits were developed with off-chip surface mount components, making it flexible for designers to use different impedance matching techniques, like stubs or quarter-wave transformers. Additionally, the characterization can be done first before the actual implementation. Moreover, off-chip components have higher quality factors than their counterparts. However, they are not widely used because it is difficult to integrate them in circuits. Modern integrated circuit technology makes it easier for designers to use on-chip components. Nevertheless, these components are limited in size and band of operation.[88]

Lumped element, transformer-based, or microstrip line matching are impedance matching techniques using on-chip components. For different applications, they have varied performance.[28,89,90]

6.1 | Lumped elements matching

Matching using lumped elements is widely used in any multiband mixer for SDR. Frequency tuning is possible by varying the resonator capacitance employing

electrostatic, piezoelectric, or thermal micro-actuators using the electrostatic technique.[91] Wang et al. proposed a matching network for a mixer operating in a high band to compensate for the effect of the parasitic capacitances seen at its IF output.[72] Likewise, peaking inductor was employed for the low band mixer to extend the IF port 3-dB bandwidth. The technique allows concurrent matching within 6–18 GHz bands. Similar work was discussed by Hashemi et al. that allows concurrent matching at 2.45 and 5.25 GHz, respectively.[92] The parallel network was proposed to resonate with both frequencies of interest. To achieve concurrent multiband gain, the drain load network should have high impedance only at frequencies of interest. This can be fulfilled by connecting a series LC branch to parallel LC tank. Each series LC branch inserts a zero into the design's gain transfer function at its series resonant frequency, which sets the frequency of the transfer function notches. This notch is intended to improve the receiver's image rejection. Likewise, Kia et al. proposed a tunable differential active inductor to tune with the parasitic capacitances.[93] The reconfiguration is possible by using a variable feedback resistor employed within the inductor. A similar approach was also discussed by Tseng et al., where lumped element-based couplers are employed to obtain different inputs.[94] The overall design consumed low power and required small die area. The design also achieved good port isolation.

6.2 | Transformer-based matching

Transformer matching can be used in multiband front-ends, among which multitap transformers proved as a better solution compared to other transformer-based approaches. Although the design is quite flexible, it may degrade the quality factor.[95] Yu et al. employed a transformer is at the output end for differential to single-ended signal conversion for wideband matching.[96] The design also employs coupling capacitors for amplitude and phase matching of the transformer. Likewise, Hermann et al. employed an on-chip resonating transformer to attain high current gain.[97] The proposed design featured a small die area and achieved good port isolation. Additionally, Tiebout et al. discussed a single-balanced transformer-based mixer topology and maintained good port isolation with small die area.[98]

6.3 | Microstrip line matching

Microstrip line-based matching is another potential approach for reconfigurable multiband mixers. Wu et al. used a T-shaped transmission lines.[99] To enhance the bandwidth, a modified Marchand balun is proposed. The proposed design covered a small area and better port isolation. However, it has limited application scenarios. Likewise, Lin et al. used a thin film microstrip line for matching networks within the circuitry and the design attained high port isolation.[100] Seyedhosseinzadeh et al. used series transmission lines to form a -shaped network in both RF and LO stages of the mixer for wideband operation.[101] The design covered a small area and achieved high CG.

7 | COMPARATIVE STUDY

Table 3 summarizes the different mixer designs related to SDRs. Each mixer topology operates within a wideband. From Table 3, most of the works have been implemented in 180 nm CMOS technology. High performance was achieved by using switching[109,116] and multi-gated transistor technique.[107]

In Table 3, the highest NF is as less as 1.5 dB and the maximum IIP3 is 12.5 dBm. Besides, reconfigurable mixers are more linear than concurrent mixers. As CG increases, the overall power dissipation increases, which degrades the IIP3 performance. The overall mixer circuit area depends on the design complexity.

8 | DESIGN CHALLENGES AND TECHNIQUES

Multiband mixer design is complex and requires a large number of passive components. Thus, it often leads to high power consumption and large chip area due to their size.[25,110] Improper mixer design may cause an imbalance among different performance metrics.[103,110,120] Therefore, different techniques have been proposed in the literature while considering the flexibility within the mixer and their wideband operation.[121] This section discusses some of the common challenges in designing such mixers and the corresponding techniques used to overcome these problems.

8.1 | Image rejection

Desired and image signals enter together at the input and degrade the performance of a mixer. Therefore, it is important to reject the image signals. Recently, it was found that RF sampling can be used as downconverters, where a discrete-time structure is more advantageous compared to the continuous-time structure. However, samplers in wideband SDRs will affect their performance. For example, the charge sampling approach shows the

TABLE 3 Comparison table

Reference	Freq (GHz)	Category	Results				
			CG/CL (dB)	NF (dB)	IIP3 (dBm)	Area (mm^2)	P_{diss} (mW)
1	57–66	Wideband	>5.6	<10.91	>12.4	0.22	18
26	5–6	Wideband	9	11	2	0.8	4.2
102	0.5–6.5	Wideband	10	13	9.5	0.015	4.5
103	1–6	Wideband	10–13	12–18	−4.5	Nil	Nil
104	3.1–10.6	Wideband	12	4–5.7	−14	0.928	4.6
105	0.7–2.3	Wideband	21	10.6	9	0.19	9.9
106	20–32	Wideband	3	10.5–13	>0.5	0.19	18
107	0.045–2.5	Wideband	5.8–8.6	7.4–9.1	0.6–7.2	0.093	16.38
2	0.01–2	Reconfigurable	17.5	11.1	−0.9	0.071	4.6
42	0.15–1	Reconfigurable	48	3.2	−7	0.72	64
108	57–64	Reconfigurable	23	9	Nil	Nil	319
109	4–10	Reconfigurable	15.5–17.5, 13.5	4–5.2	12.5	Nil	8.3
110	0.401–0.457	Reconfigurable	29–31	<5.2	>−19.5	0.6	0.37
111	1.4–3.6	Reconfigurable	12.3	16.9	4.8	4.6	Nil
112	1.5–4.5	Reconfigurable	12–16.4	8.2–12	−11	0.919	0.28
113	0.1–5	Reconfigurable	68–84	2.3–6.5	−3 to 10	2	59–115
114	0.1–2.4	Reconfigurable	40–70	−4+/−1	Nil	2.5	37–70
115	2–3	Reconfigurable	33	11	−16	0.1	2.5
116	1–2	Reconfigurable	29.4–92.6, 15.8–20.1	4.9, 14.8	0.9	Nil	46.4, 67.3
72	6–18	Concurrent	31	12	−11	Nil	137.6
117	0.3–1.4	Concurrent	42	2.5–3.9	Nil	0.48	Nil
54	0.8–1, 1.8–2	Concurrent	19.3–20, 19.2–20.2	1.85–1.95, 1.55–1.85	−3, −4.5	Nil	67.5
118	2.3, 5.2	Concurrent	15.6, 11.3	12.1, 16	−6.7, −1.1	Nil	7.52
119	3.1–4.8, 6.3–7.9	Concurrent	12.5–16.5, 14.5–16	7.5–12.5	−4.1, −5.2	1.02	75.6

Abbreviations: CG, conversion gain; IIP3, third-order input intercept point; NF, noise figure.

inverse CG and frequency relation. Although this issue was resolved with voltage samplers, wideband noise folding occurs with this sampling process. Therefore, prefiltering is required in both cases.[122] However, this approach not only is difficult to implement, but also increases the overall cost of the receiver as well as the design complexity.[123] Hence, the best way is to design an image rejected mixer that will reduce the overall receiver complexity, while enhancing its reliability and performance.[124–127] Gong et al. proposed mage rejection mixers, which is a combination of a single-balanced mixer and the orthogonal bridge.[125] The design has attained an acceptable IRR, but the conversion loss is increased.

8.2 | Conversion gain-linearity balance

Modern transceivers are developed using CMOS process technologies due to their ability to provide low-cost design and low-power consumption.[128] However, CMOS transistors have a low transconductance that automatically degrades the CG. Hence, supplementary amplifiers are required to compensate for the low CG.[120] Cascode current bleeding and g_m-boosting techniques are well known for CG improvement. These techniques are beneficial if the low chip area is required. Nevertheless, these techniques may not guarantee good IIP3,[120,129,130] which clearly illustrates the gain-linearity trade-off. Na et al. proposed a mixer with a current mirror approach, which attained low NF, high CG at the expense of IIP3.[131]

8.3 | Power consumption

The recent development of mobile communication devices has witnessed an ever-increasing level of circuit integration. This advancement would have been incomprehensible without a device downscaling process that further leads to performance improvement. The latest research focuses on the system-on-chip. The CMOS technology faces challenges in achieving continued downscaling of power consumption while satisfying the development trend of software-defined radios for modern wireless communications.[132] It has been found that CMOS wideband mixers consume low power.[133,134] However, it degrades other performance metrics.[60,115,129,135] Moreover, CCPT, inductive peaking, and current bleeding approaches were used for high CG, low-power utilization, but these approaches also degraded the linearity.[136] Likewise, Bazrafshan et al. showed that the use of cascode common source approach is useful for low-power consumption.[10] Similar works were discussed by researchers that consumed low power but at the expense of other performance metrics.[10,60,66,129,135,137,138]

8.4 | Noise performance

Several techniques are available to reduce the NF of mixers. One of the most common approaches is to adopt filters. For example, Hu et al. proposed a wideband tunable Gilbert mixer using an appropriate filter that attained a moderate NF with low-power consumption at the expense of overall die area.[16]

Cordova et al. used a dynamic current injection approach along with the filters attaining a moderate NF.[39] Likewise, Gladson et al. proposed a mixer that operates in two modes, that is, high gain mode and high linearity mode for low rate wireless personal area network applications.[66] The proposed design in high gain mode attained high CG, low IIP3, and moderate NF. On the contrary, its high linearity mode attained high IIP3,

TABLE 4 Proposed approaches and future scope comparison table

Type of mixer	Objective	Proposed technique	Future scope
Reconfigurable	Gain-linearity trade-off	Passive inductors based tunable resonator[16]	Use of active inductors
Concurrent		Balanced LNA-mixer structure[54]	Linearity improvement
Concurrent	Power consumption	Dual matching network[47]	Increasing the overall operating band
Reconfigurable		Receiver with programmable notches[10]	Linearity improvement
Reconfigurable		Current driven passive mixer[74]	Maintaining a good trade-off among power and other metrics
Reconfigurable	Image rejection	Discrete-time mixing[122]	Improving CG
Concurrent	Noise performance	Current-reuse source degeneration MGTR[59]	Improving CG

Abbreviations: CG, conversion gain; MGTR, multiple gated transistor.

moderate CG, and high NF. Therefore, a single design cannot operate in both modes that can attain high gain and linearity simultaneously. Both designs had a moderate NF, limited IIP3 and CG in different modes.

9 | SUMMARY AND PROSPECTIVE DEVELOPMENT

Through the detailed literature survey, we notice that techniques may vary depending on the applications and requirements. Indeed, it is quite challenging to balance the trade-offs among different parameters when designing mixers for SDRs. Common mixer design techniques are current bleeding,[120,139–141] active balun,[87] current mirror,[142] gain boosting,[129] current reuse,[135] and current injection,[102] double linearizations.[143] In general, the selection of a particular technique depends on the performance optimization goal for the mixer design as every technique has its benefits, however, there are some associated drawbacks as well. Great care must be taken while opting for a particular technique. This information together with the aforementioned literature study provides ample opportunity for further investigations in the design of mixers.

This section not only summarizes the survey but also discusses the prospects of mixer design based on the design problems as summarized in Table 4. Based on this survey, we take the liberty to provide some general advice for implementing multiband or wideband mixers as follows:

1. Wideband or multiband mixers can be used as a part of SDR receiver circuitry to enclose the complete desired frequency band compared to narrowband mixers to overcome the need of several receivers capable of covering different frequency bands. Fully balanced mixer structures can be used to eliminate even-order distortion within the receiver circuitry.
2. Impedance matching plays an important role for simultaneous reconfiguration while proposing reconfigurable multiband mixers. Lumped element-based matching is suitable for low-frequency bands, and microstrip line-based matching is required for high-frequency bands, which may increase the overall chip area and power consumption.
3. Most works in the literature with low-power consumption and chip area operate within single frequency bands. However, it is difficult for multiband mixers to achieve low-power operation as they require complex matching circuits, which unavoidably increases the power consumption and circuit area of the design. Additionally, extra care is required for the parasitics handling as they might affect the input impedance, in turn affecting the overall CG and NF performance.

ACKNOWLEDGMENT

The authors would like to thank both universities for providing us the platform to research and contribute toward this study. This work received no external funding.

CONFLICT OF INTEREST

The authors declare no conflict of interest.

DATA AVAILABILITY STATEMENT

Data sharing is not applicable to this article as no new data were created or analyzed in this study.

ORCID

Shilpa Mehta https://orcid.org/0000-0002-4691-3185

REFERENCES

1. Choi C, Son JH, Lee O, Nam I. A +12-dBm OIP3 60-GHz RF downconversion mixer with an output-matching, noise- and distortion-canceling active balun for 5G applications. *IEEE Microw Wirel Compon Lett*. 2017;27:284-286.
2. Li M, Zhigong W, Jian X. A 1-V current-reused wideband current-mirror mixer in 180-nm CMOS with high IIP2. *Circuits Syst Signal Process*. 2017;36:1806-1817.
3. Douss S, Touati F, Loulou M. Design optimization methodology of CMOS active mixers for multi-standard receivers. *Int J Electron Commun Eng*. 2007;1:1328-1336.
4. Maja V. *Configurable Circuits and their Impact on Multi-Standard RF Front-End Architectures*. Thesis. Eindhoven University of Technology; 2011.
5. Yoon J, Kim H, Park C, et al. A new RF CMOS gilbert mixer with improved noise figure and linearity. *IEEE Trans Microw Theory Tech*. 2008;56:626-631.
6. Mannar MP. *Framework for the Design and Implementation of Software Defined Radio Based Wireless Communication System*. Thesis. University of Akron; 2005.
7. Haldren HA. *Studies in Software-Defined Radio System Implementation*. Thesis. Liberty University; 2014.
8. Cruz P, Carvalho NB, Remley KA. Designing and testing software-defined radios. *IEEE Microw Mag*. 2010;11:83-94.
9. Zamat H, Nassar CR. Introducing software defined radio to 4G wireless: necessity, advantage, and impediment. *J Commun Netw*. 2002;4:1-7.
10. Bazrafshan A, Taherzadeh-Sani M, Nabki F. A 0.8–4-GHz software-defined radio receiver with improved harmonic rejection through non-overlapped clocking. *IEEE Trans Circuits Syst I Regul Pap*. 2018;65:3186-3195.
11. Fei G. *Front End Circuit Module Designs for A Digitally Controlled Channelized SDR Receiver Architecture*. Thesis. Electrical and Computer Engineering, The Ohio State University; 2011.
12. Liu X, Wang Z, Deng Q. Design and FPGA implementation of a reconfigurable 1024-channel channelization architecture for

SDR application. *IEEE Trans Very Large Scale Integr VLSI Syst*. 2016;24:2449-2461.
13. Singh TV, Vimal B. Low cost and power software defined radio using raspberry pi for disaster effected regions. *Proc Comput Sci*. 2015;58:401-407.
14. Rohde S. Software defined radios – overview and hardware (1) The Rohde and Schwarz News Magazine; 2004:58–61.
15. Ching LW, Fung TK, Yi S, Tai CK. A current bleeding CMOS mixer featuring LO amplification based on current-reused topology. *Circuits Syst*. 2013;4:58-66.
16. Xin H. *RF CMOS Tunable Gilbert Mixer with Wide Tuning Frequency and Controllable Bandwidth: Design Sythesis and Verification*. Thesis. Wright State University; 2017.
17. Asad Bashar ZJ. *Low-Noise 24 GHz 0.15um GaAs pHEMT Gilbert Cell Mixer for Intelligent Transportation System Radar Receiver*. Thesis. University of Ottawa; 2014.
18. Hank Z. *Linear Circuit Design Handbook*. Elsevier; 2008.
19. Siddiqi AA. *Design Methodology and Investigation of GHz Range CMOS RF Mixers*. Thesis. Carleton University; 2000.
20. Maity B, Sethy PK, Bandyopadhyay K. Design of a single balanced diode mixer with high LO/RF and LO/IF isolation in C-band test loop translator. Paper presented at: 2012 IEEE International Conference on Advanced Communication Control and Computing Technologies (ICACCCT):14–17; 2012.
21. MicrowavesIOI. Mixers; 2011.
22. Mini-Circuits. Novel Passive FET Mixers Provide Superior Dynamic Range; 2015.
23. Rahul S, Abhay C, Manish K. A comparative study of different types of mixer topologies. *ICTACT J Microelectron*. 2016;2:182-187.
24. Tiwari S, Manjula J. Performance analysis of 1.8 GHz to 5 GHz HEMT multiband mixer. *Int J Appl Eng Res*. 2016;11:6312-6317.
25. Dongfang P, Zongming D, Huang L, et al. Design of high-linearity 75–90 GHz CMOS down-conversion mixer for automotive radar. *Analog Integr Circuits Signal Process*. 2018;97:313-322.
26. Marko K, Georg B. A broadband folded Gilbert cell CMOS mixer. *Analog Integr Circuits Signal Process*. 2010;64:39-44.
27. Almohaimeed AM, Yagoub MCE. Efficient current bleeding mixer for WiMax applications. *AASRI Proc*. 2014;9:92-98.
28. Fan X, Gu C, Tao J, Hua Z. A reconfigurable 0.7–2.6GHz wideband mixer for multi-mode multi-standard receivers in 0.18um RF CMOS. Paper presented at: IEEE MTT-S International Microwave Workshop Series on Advanced Materials and Processes for RF and THz Applications (IMWS-AMP):1–3; 2015.
29. Bhatt D, Mukherjee J, Redouté J. Low-power linear bulk-injection mixer for wide-band applications. *IEEE Microw Wirel Compon Lett*. 2016;26:828-830.
30. Fan J, Carlos S. Codesign of mixer-VGA downconverter blocks. *Can J Electr Comput Eng*. 2015;38:199-203.
31. Yi LC, Ramiah H, Rajendran J. A triple cross coupled down-conversion mixer in 65 nm CMOS technology. Paper presented at: 2019 IEEE International Circuits and Systems Symposium (ICSyS):1–4; 2019.
32. Chrisben G, Bhaskar M, Praveen R, Sudharsan SA. 261-uW ultra-low power RF mixer with 26-dBm IIP3 using complementary pre-distortion technique for IEEE 802.15.4 applications. *AEU - Int J Electron Commun*. 2019;107:70-82.
33. Nguyen TT, Fujii K, Pham A. Highly linear distributed mixer in 0.25-um enhancement-mode GaAs pHEMT technology. *IEEE Microw Wirel Compon Lett*. 2017;27:1116-1118.
34. Henderson BC. Mixers: part 1 characteristics and performance; 2001.
35. Zhang J, Chan EHW, Wang X, Feng X, Guan B. High conversion efficiency photonic microwave mixer with image rejection capability. *IEEE Photon J*. 2016;8:1-11.
36. Pushpak A, Rayudu V. *A Reconfigurable SPICE-Based CMOS LNA Design in 90 nm Technology Using ADS RFIC Dynamic Link*. Thesis. Wright State University; 2015.
37. Zijie H, Mouthaan K. A 1- to 10-GHz RF and wideband IF cross-coupled Gilbert mixer in 0.13-um CMOS. *IEEE Trans Circuits Syst II Express Briefs*. 2013;60:726-730.
38. Technologies Copper Mountain. RF mixer characterization; 2015.
39. Cordova D, Bampi S, Fabris E. A CMOS down-conversion mixer with high IIP2 and IIP3 for multi-band and multiple standards. Paper presented at: 27th Symposium on Integrated Circuits and Systems Design (SBCCI):1–7; 2014.
40. Xin C, Shuxiang S, Mingcan C. Design and analysis of a broadband current-mode CMOS direct-conversion receiver frond-end circuit. *J Circuits Syst Comput*. 2018;28:1-23.
41. He T, Wang G, Yousef K, Jin J. A high conversion gain wideband mixer design for UWB applications. Paper presented at: 2019 IEEE International Symposium on Circuits and Systems (ISCAS):1–4; 2019.
42. Renzhi L, Lawrence P, Weldon Jeffrey A. A wideband RF receiver with extended statistical element selection based harmonic rejection calibration. *Integration*. 2016;52:185-194.
43. Nandini V, Harikrishnan R, Wei-Keat C, Tan G-H, Jeevan K, Wasif RA. 50 MHz–10 GHz low-power resistive feedback current-reuse mixer with inductive peaking for cognitive radio receiver. *Sci World J*. 2014;2014:683971.
44. Yang G, Wang K. 25-45 GHz wideband mixer with simultaneous RF- and LO-port inductive peaking technique. Paper presented at: 2018 14th IEEE International Conference on Solid-State and Integrated Circuit Technology (ICSICT):1–3; 2018.
45. Guo B, Wang H, Yang G. A wideband merged CMOS active mixer exploiting noise cancellation and linearity enhancement. *IEEE Trans Microw Theory Tech*. 2014;62:2084-2091.
46. Yo-Sheng L, Kai-Siang L. Design and implementation of a 60–113 GHz down-conversion mixer in 90Â nm CMOS. *Analog Integr Circuits Signal Process*. 2020;104:109-119.
47. Abdelrheem TA, Elhak HY, Sharaf KM. A concurrent dual-band mixer for 900-MHz/1.8GHz RF front-ends. Paper presented at: 46th Midwest Symposium on Circuits and Systems: 1291–1294; 2003.
48. Hsu H, Duan Q, Liao Y. A low power 2.4/5.2GHz concurrent receiver using current-reused architecture. Paper presented at: IEEE International Symposium on Circuits and Systems (ISCAS):1398–1401; 2016.
49. Namrata Y, Abhishek P, Vijay N. Design of low voltage Integrated CMOS RF front-end based LNA and mixer for GPS application. *Mater Today: Proc*. 2017;4:10362-10366.

50. Abhay C, Mithilesh K, Dr M. A high gain low noise figure double balanced down conversion mixer for band 1 of WiMedia system Indian. *J Sci Technol*. 2019;12:1-14.
51. Chi YL, Harikrishnan R, Nandini V, Jagadheswaran R. A 2.4 mW, +11.3 dBm IIP3 and 17Â dB conversion gain CMOS mixer with capacitor cross-coupled and modified post distortion techniques. *AEU - Int J Electron Commun*. 2020;123:153246.
52. Mazor N, Sheinman B, Katz O, et al. Highly linear 60-GHz SiGe downconversion/upconversion mixers. *IEEE Microw Wirel Compon Lett*. 2017;27:401-403.
53. Gupta SK, Yadava N, Chauhan RK. Gilbert mixer cell design for RF application using CMOS technology. Paper presented at: 2019 IEEE 5th International Conference for Convergence in Technology (I2CT):1–6; 2019.
54. Adiseno IM, Olsson H. A wide-band RF front-end for multiband multistandard high-linearity low-IF wireless receivers. *IEEE J Solid-State Circuits*. 2002;37:1162-1168.
55. Belkhiri C, Toutain S, Razban T. Wide bandwidth and low power CMOS mixer with high linearity for multiband receivers using direct conversion implementation. Paper presented at: The European Conference on Wireless Technology, 2005:269–272; 2005.
56. Pouya S, Mohammad Y. A wideband high linearity and low-noise CMOS active mixer using the derivative superposition and noise cancellation techniques. *Circuits Syst Signal Process*. 2019;38:2910-2930.
57. Blaakmeer SC, Klumperink EAM, Leenaerts DMW, Nauta B. The blixer, a wideband balun-LNA-I/Q-mixer topology. *IEEE J Solid-State Circuits*. 2008;43:2706-2715.
58. Hamed KW, Freundorfer AP, Antar YMM. A monolithic double-balanced direct conversion mixer with an integrated wideband passive balun. *IEEE J Solid-State Circuits*. 2005;40:622-629.
59. Chen Y, Yan N, Xu J, Chen Q, Sun J. Low power, high linearity multi-mode downconversion mixer for SDR. Paper presented at: IEEE International Symposium on Circuits and Systems (ISCAS):737–740; 2013.
60. Lee CJ, Kang J, Park CS. A D -band low-power gain-boosted up-conversion mixer with low LO power in 40-nm CMOS technology. *IEEE Microw Wirel Compon Lett*. 2017;27:1113-1115.
61. Liu T. Y., Liscidini A.. 20.9 A 1.92mW filtering trans-impedance amplifier for RF current passive mixers. Paper presented at: 2016 IEEE International Solid-State Circuits Conference (ISSCC):358–359; 2016.
62. Ko J, Gharpurey R. A pulsed UWB transceiver in 65 nm CMOS with four-element Beamforming for 1 Gbps meter-range WPAN applications. *IEEE J Solid-State Circuits*. 2016;51:1177-1187.
63. Murphy D, Hafez A, Mirzaei A, et al. A blocker-tolerant wide-band noise-cancelling receiver with a 2dB noise figure. Paper presented at: 2012 IEEE International Solid-State Circuits Conference:74–76; 2012.
64. Kim N, Aparin V, Larson LE. A resistively degenerated wide-band passive mixer with low noise figure and +60dBm IIP2 in 0.18um CMOS. Paper presented at: 2008 IEEE Radio Frequency Integrated Circuits Symposium:185–188; 2008.
65. Lin Y, Lan K, Wang C, Chi C, Lu S. 6.3 mW 94 GHz CMOS down-conversion mixer with 11.6 dB gain and 54 dB LO-RF isolation. *IEEE Microw Wirel Compon Lett*. 2016;26:604-606.
66. Chrisben G, Bhaskar M. A low power high-performance area efficient RF front-end exploiting body effect for 2.4GHz IEEE 802.15.4 applications. *AEU - Int J Electron Commun*. 2018;96:81-92.
67. Vojkan V, Arjan L, Tang J. *Adaptive Multi-Standard RF Front-Ends*. Springer; 2008.
68. He Q, Liu Y, Li S, Yu C, Liu X, Wu Y. The concurrent dual-band receiver architecture with one mixer. Paper presented at: Third Pacific-Asia Conference on Circuits, Communications and System (PACCS):1–4; 2011.
69. Heragu A, Balasubramanian V, Enz C. A concurrent quadrature sub-sampling mixer for multiband receivers. Paper presented at: European Conference on Circuit Theory and Design:271–274; 2009.
70. Jou CF, Cheng K-H, Lien W-C, Wu CH, Yen CH. Design of a concurrent dual-band receiver front-end in 0.18 um CMOS for WLANs Paper presented at: IEEE 802.11a/b/g applications in 47th Midwest Symposium on Circuits and Systems;1:177–180; 2004.
71. Chen P-D, Chen C-H, Chang W-M, Cheng K-H, Jou CF. A dual-band concurrent RF front-end receiver design for GPS and Bluetooth applications. Paper presented at: Asia-Pacific Microwave Conference:1–4; 2005.
72. Wang R-L, Su Y-K, Liu CH, Hung S-C, Yang P-J,Lin Y-S. A concurrent dual-band mixer with on-wafer balun for multi-standard applications. Paper presented at: IEEE Asia Pacific Conference on Circuits and Systems;2008:304–307.
73. Vahidfar MB, Shoaei O, Svelto F. A high dynamic range multi-standard CMOS mixer for GSM, UMTS and IEEE802.11b-g-a applications. Paper presented at: IEEE Radio Frequency Integrated Circuits Symposium:193–196; 2008.
74. Cao M, Chi B, Zhang C, Wang Z. A 1.2V 0.1–3GHz software-defined radio receiver front-end in 130nm CMOS. Paper presented at: IEEE Radio Frequency Integrated Circuits Symposium:1–4; 2011.
75. Manen L v, Klumperink EAM, Cornelissens K, Borremans M, Nauta B. A switched capacitor digital sinewave mixer for software-defined radio. *IEEE Solid-State Circuits Lett*. 2019;2:13-16.
76. Ashish K, Samaresh B, Manish N, Phani K. Front-end digital signal processing scheme for 206.5 MHz atmospheric radar application. *Int J Adv Dent Tech*. 2011;2:71-81.
77. Mostafa I, Islam G. Improved SDR frequency tuning algorithm for frequency hopping systems. *ETRI J*. 2016;38:455-462.
78. Angsuman R. FPGA-based applications for software radio signal processing; 2004:24–35.
79. Ye Z, Grosspietsch J, Memik G. An FPGA based all-digital transmitter with radio frequency output for software defined radio. Paper presented at: 2007 Design, Automation and Test in Europe Conference and Exhibition:1–6; 2007.
80. Wu L, Ng AWL, Zheng S, et al. A 0.9–5.8-GHz software-defined receiver RF front-end with transformer-based current-gain boosting and harmonic rejection calibration. *IEEE Trans Very Large Scale Integr VLSI Syst*. 2017;25:2371-2382.

81. Xinwang Z, Zipeng C, Yanqiang G, et al. A 0.1–5.0 GHz flexible SDR receiver with digitally assisted calibration in 65 nm CMOS. *Microelectron J*. 2018;72:58-73.
82. Qin P, Xue Q. A low-voltage folded-switching mixer using area-efficient CCG transconductor. *IEEE Trans Circuits Syst II Express Briefs*. 2017;64:877-881.
83. Yang D, Yüksel H, Newman C, et al. A fully integrated software-defined FDD transceiver tunable from 0.3-to-1.6 GHz. Paper presented at: IEEE Radio Frequency Integrated Circuits Symposium (RFIC):334–337 2016.
84. Sowlati T, Agarwal B, Cho J, et al. Single-chip multiband WCDMA/HSDPA/HSUPA/EGPRS transceiver with diversity receiver and 3G DigRF interface without SAW filters in transmitter / 3G receiver paths. Paper presented at: 2009 IEEE International Solid-State Circuits Conference - Digest of Technical Papers:116–117, 117a; 2009.
85. Poobuapheun N, Chen W, Boos Z, Niknejad AM. A 1.5-V 0.7–2.5-GHz CMOS quadrature demodulator for multiband direct-conversion receivers. *IEEE J Solid-State Circuits*. 2007;42:1669-1677.
86. Rui G, Haiying Z. A multi-mode multi-band RF receiver front-end for a TD-SCDMA/LTE/LTE-advanced in 0.18-um CMOS process. *J Semiconduct*. 2012;33:095003.
87. Nguyen TT, Fujii K, Pham A. A 7–42 GHz dual-mode reconfigurable mixer with an integrated active IF balun. Paper presented at: 2017 IEEE MTT-S International Microwave Symposium (IMS):2018–2021; 2017.
88. Salmeh R. Impacts of impedance mismatch on the performance of RF mixers. Paper presented at: 2011 IEEE Symposium on Wireless Technology and Applications (ISWTA):27–31; 2011.
89. Chironi V, Pasca M, Siciliano P, Amico SD'. A 5.8–13 GHz SDR RF front-end for wireless sensors network robust to out-of-band interferers in 65nm CMOS. Paper presented at: 6th International Workshop on Advances in Sensors and Interfaces (IWASI):137–140; 2015.
90. Oh H, Kim J, Lim J, Kim C. A 2.4-GHz high conversion gain passive mixer using Q -boosted pi -type LCL matching networks in 90-nm CMOS. *IEEE Microw Wirel Compon Lett*. 2017;27:736-738.
91. Rais-Zadeh M, Fox JT, Wentzloff DD, Gianchandani YB. Reconfigurable radios: a possible solution to reduce entry costs in wireless phones. *Proc IEEE*. 2015;103:438-451.
92. Hamed H. *Integrated Concurrent Multi-band Radios and Multiple-antenna Systems*. Thesis. Institute of Technology 2003.
93. Babaei KH, Khari A'a A. A high gain and low flicker noise CMOS mixer with low flicker noise corner frequency using tunable differential active inductor. *Wirel Pers Commun*. 2014;79:599-610.
94. Tseng SC, Meng C, Huang GW. SiGe BiCMOS subharmonic Gilbert mixer using lumped-element rat-race couplers. *Microw Opt Technol Lett*. 2007;49:2018-2020.
95. Xiaohua Y. *Design of reconfigurable multi-mode RF circuits*. Thesis. Iowa State University; 2013.
96. Yu J, Jixin C, Huanbo L, et al. Transformer matched gilbert mixer with active balun for D band transmitter. *Microw Opt Technol Lett*. 2019;62:1-7.
97. Hermann C, Tiebout M, Klar H. A 0.6V 1.6mW transformer based 2.5GHz downconversion mixer with +5.4dB gain and −2.8dBm IIP3 in 0.13 um CMOS. Paper presented at: 2004 IEE Radio Frequency Integrated Circuits (RFIC) Systems. Digest of Papers:35–38; 2004.
98. Tiebout M, Liebermann T. A 1V fully integrated CMOS transformer based mixer with 5.5dB gain, 14.5dB SSB noise figure and 0dBm input IP3 in ESSCIRC 2004 - 29th European Solid-State Circuits Conference (IEEE Cat. No03EX705):577–580; 2004.
99. Wu Y, Hwang Y, Chiong C, Lu B, Wang H. A 40-nm CMOS mixer with 36-GHz IF bandwidth and 60–148 GHz RF passband. Paper presented at: 2019 IEEE Asia-Pacific Microwave Conference (APMC):57–59; 2019.
100. Lin C, Wu P, Chang H, Wang H. A 9-50-GHz Gilbert-cell down-conversion mixer in 0.13-um CMOS technology. *IEEE Microw Wirel Compon Lett*. 2006;16:293-295.
101. Neda S, Abdolreza N, Sona C, Simon HZ, Mingquan B, Herbert Z. A SiGe high gain and highly linear F-band single-balanced subharmonic mixer. *Zonedo*. 2017;1-4.
102. Mohsenpour M, Saavedra CE. Method to improve the linearity of active commutating mixers using dynamic current injection. *IEEE Trans Microw Theory Tech*. 2016;64:4624-4631.
103. Darshak B, Jayanta M, Jean-Michel R. A self-biased mixer in 0.18um CMOS for an ultra-wideband receiver. *IEEE Trans Microw Theory Tech*. 2017;65:1294-1302.
104. Hsu Meng-Ting W, Kun-Long CW-C. Systematic approaches of UWB low-power CMOS LNA with body biased technique. *Wirel Eng Technol*. 2015;06:61-77.
105. Bao K, Fan X, Li W, Wang Z. A wideband current-commutating passive mixer for multi-standard receivers in a 0.18 um CMOS. *J Semicond*. 2013;34:1-9.
106. Mohamed E-N, Sanchez-Sinencio E, Entesari Kamran A. 20–32-GHz wideband mixer with 12-GHz IF bandwidth in 0.18-um SiGe process. *IEEE Trans Microw Theory Tech*. 2010;58:2731-2740.
107. Liu L, Zhang K, Ren Z, Zou X, Lu Z, Liu D. Wideband CMOS mixer using differential circuit transconductance linearization technique in IEEE International Symposium on Radio-Frequency Integration Technology (RFIT):121–123; 2015.
108. Nasr I, Jungmaier R, Baheti A, et al. A highly integrated 60 GHz 6-channel transceiver with antenna in package for smart sensing and short-range communications. *IEEE J Solid-State Circuits*. 2016;51:2066-2076.
109. Hao L. *Advanced Downconversion Mixers for CMOS Radio Frequency Integrated Circuits*. Thesis. Queen's University; 2017.
110. Choi C, Kwon K, Nam I. A 370 um CMOS MedRadio receiver front-end with inverter-based complementary switching mixer. *IEEE Microw Wirel Compon Lett*. 2016;26:73-75.
111. Wei H-C, Hsiao C-L. A 1 V bulk-controlled gm-boosted CMOS mixer for LTE-A applications. Paper presented at: IEEE 2nd Global Conference on Consumer Electronics:239–242; 2013.
112. Nandini V, Harikrishnan R, Balan Zechariah A. 350Â mV, 280Â uW 1.5-to-4.5-GHz wideband folded mixer adopting capacitive-cross-plus-magnetic-coupling. *AEU - Int J Electron Commun*. 2020;119:153174.
113. Giannini V, Nuzzo P, Soens C, et al. A 2-mm^2 0.1–5 GHz software-defined radio receiver in 45-nm digital CMOS. *IEEE J Solid-State Circuits*. 2009;44:3486-3498.

114. Caroline A, Alyosha M. A passive mixer-first receiver with digitally controlled and widely tunable RF interface. *IEEE J Solid-State Circuits*. 2011;45:2696-2708.
115. Chen C, Wu J. A 1.2-V self-reconfigurable recursive mixer with improved IF linearity in 130-nm CMOS. *IEEE Trans Circuits Syst II Express Briefs*. 2017;64:36-40.
116. Guan R, Jin J, Pan W, Chen D, Zhou J. Wideband dual-mode complementary metal_oxide_semiconductor receiver. *IET Circuits Dev Syst*. 2016;10:87-93.
117. Agrawal A, Natarajan A. A concurrent dual-frequency/angle-of-incidence spatio-spectral notch filter using Walsh function passive sequence mixers. Paper presented at: 2017 IEEE MTT-S International Microwave Symposium (IMS):1606–1609; 2017.
118. Wang Ruey-Lue S, Yan-Kuin CH-H, et al. A concurrent dual-band folded-cascode mixer using a LC-tank biasing circuit. *Microelectron J*. 2012;43:1010-1015.
119. Chirala MK, Cam N. A CMOS fully integrated concurrent dual ultrawideband receiver frontend. *Microw Opt Technol Lett*. 2009;51:2003-2007.
120. Ji-Young L, Tae-Yeoul Y. A dynamic current-bleeding technique for a low-noise and high-gain CMOS mixer. *Microw Opt Technol Lett*. 2017;59:1267-1271.
121. Huang C, Wu K, Hu R, Chang C. Analysis of wide-IF-band 65-nm-CMOS mixer for 77–110-GHz radio-astronomical receiver design. *IET Circuits Dev Syst*. 2019;13:406-413.
122. Zhiyu R, Eric K, Bram N. A discrete-time mixing receiver architecture with wideband image and harmonic rejection for software-defined radio Electronic Notes in Theoretical Computer Science – ENTCS; 2008.
123. Mollaalipour M, Miar-Naimi H. Design and analysis of a highly efficient linearized CMOS subharmonic mixer for zero and low-IF applications. *IEEE Trans Very Large Scale Integr VLSI Syst*. 2016;24:2275-2285.
124. Azevedo F, Rosario MJ, Freire JC. CMOS monolithic wide-band image rejection mixer with poly_phase filters. Paper presented at: IEEE MTT-S International Microwave and Optoelectronics Conference:815–818; 2003.
125. Gong J, Lei M, Wang Y, Li Y. The design of image rejection mixer in W-band in 16th International Conference on Electronic Packaging Technology (ICEPT):22–24; 2015.
126. Li YC, Xue Q. Wide band receiver with high image rejection using 0.18 um CMOS technology. Paper presented at: IEEE International Workshop on Electromagnetics: Applications and Student Innovation Competition:1–3; 2016.
127. Liang C, Rao P, Huang T, Chung S. A 2.45/5.2 GHz image rejection mixer with new dual-band active notch filter. *IEEE Microw Wirel Compon Lett*. 2009;19:716-718.
128. Roy A, Harun-ur Rashid ABM. Design of a low power compensated 90nm RF multiplier with improved isolation characteristics for a transmitted reference receiver front end. *World Acad Sci Eng Technol*. 2011;80:743-749.
129. Lee CJ, Park CS. A D-band gain-boosted current bleeding down-conversion mixer in 65 nm CMOS for Chip-to-Chip communication. *IEEE Microw Wirel Compon Lett*. 2016;26:143-145.
130. Giovanni P, Claudio T, Avitabile G, Giuseppe C. Gilbert cell mixer design based on a novel systematic approach for nano-scale technologies. Paper presented at: IEEE 18th Wireless and Microwave Technology Conference (WAMICON):1–4; 2017.
131. Na D, Kim TW. A 1.2 V, 0.87–3.7 GHz wideband low-noise mixer using a current Mirror for multiband application. *IEEE Microw Wirel Compon Lett*. 2012;22:91-93.
132. Boeck G. Design of RF-CMOS integrated circuits for wireless communications. Paper presented at: 2008 National Radio Science Conference:1–8; 2008.
133. Zhang Y, Liang W, Sakalas P, et al. 12-mW 97-GHz low-power downconversion mixer with 0.7-V supply voltage. *IEEE Microw Wirel Compon Lett*. 2019;29:279-281.
134. Shubham K, Satyam S, Kumar DS, Pal S, Aminul I. A 2.4Â GHz double balanced downconversion mixer with improved conversion gain in 180-nm technology. *Microsyst Technol*. 2020;26:1721-1731.
135. Cruz H, Huang H, Lee S, Luo C. A 1.3 mW low-IF, current-reuse, and current-bleeding RF front-end for the MICS band with sensitivity of −97 dbm. *IEEE Trans Circuits Syst I Regul Pap*. 2015;62:1627-1636.
136. Lin Y, Wang YE. Design and analysis of a 94-GHz CMOS down-conversion mixer with CCPT-RL-based IF load. *IEEE Trans Circuits Syst I Regul Pap*. 2019;66:3148-3161.
137. Kim C, Joshi S, Thomas CM, Ha S, Larson LE, Cauwenberghs G. A 1.3 mW 48 MHz 4 channel MIMO baseband receiver with 65 dB harmonic rejection and 48.5 dB spatial signal separation. *IEEE J Solid-State Circuits*. 2016;51:832-844.
138. Yo-Sheng L, Kai-Siang L, Chien-Chin W, Guo-Hao L. Design and implementation of a 94 GHz CMOS down-conversion mixer with integrated miniature planar baluns for image radar sensors. *Analog Integr Circuits Signal Process*. 2017;91:353-365.
139. Yo-Sheng L, Kai-Siang L. A W-band CMOS down-conversion mixer using CMOS-inverter-based RF GM stage for conversion gain and linearity enhancement. *Analog Integr Circuits Signal Process*. 2019;99:133-146.
140. Lee J, Yun T. Low-flicker-noise and high-gain mixer using a dynamic current-bleeding technique. *IEEE Microw Wirel Compon Lett*. 2017;27:733-735.
141. Ji-Young L, Tae-Yeoul Y. High-gain mixer using cascode current bleeding and gm-boosting techniques. *Microw Opt Technol Lett*. 2017;59:1-6.
142. Kalamani C. Design of differential LNA and double balanced mixer using 180 nm CMOS technology. *Microprocess Microsyst*. 2019;71:1-9.
143. Chrisben GS, Vijayalakshmi S, Sowmya LM, Bhaskar M. Linearity improvement of RF mixer using double-linearization for 5 GHz applications. *AEU - Int J Electron Commun*. 2019;110:152856.

How to cite this article: Mehta S, Li XJ, Donelli M. Recent advancement in the design of mixers for software-defined radios. *Int J RF Microw Comput Aided Eng*. 2022;32(2):e22963. doi:10.1002/mmce.22963